

# Investigation and Measurement of a Sea Water Antenna Array

Timi Adeyemi, Kris Buchanan, and Carlos Flores

Electromagnetics Technology Branch  
Space and Naval Warfare Systems Center Pacific (SSC Pacific)  
San Diego, CA 92152, USA

**Abstract**—This work examines the behavior of a two-element sea water antenna array. A basic transmission formulation is introduced first to understand the mechanisms of the sea water phased array antenna. We then present a brief overview of phased array theory, followed by a discussion of the design and resulting measurements. Numerical simulations are compared to measured data to show the generation of sum beam radiation patterns.

**Keywords**— *Antenna array, collaborative beamforming, distributed beamforming, phased array, random array, sea water antenna, and wireless sensor networks*

## I. INTRODUCTION

A sea water antenna can be constructed by pushing a stream of conducting liquid through a ferromagnetic ring. The water stream acts as a radiator, while the ferromagnetic ring couples the energy picked up by the stream. Sea water antennas possess a number of exclusive qualities not inherent to traditional antennas [1-2]. These unique properties include reduced footprint for lower probability of detection and intercept, multiband capabilities due to its frequency diversity as a function of the height and width of the seawater stream, and lower cost due to the elimination of metallic structures. When used in a distributed array, a sea water antenna's multifunctionality and integrated value can be observed in communications, data-links, radar (search and track), and electronic warfare (EW) applications.

## II. TRANSMISSION LINE BEAMSTEERING

To establish the basic technique of transmission lines, consider an electromagnetic wave of frequency  $f$  propagating through a transmission line of length  $l$  with a velocity of  $v$ . The electromagnetic wave experiences a phase shift as follows:

$$\phi = kl = 2\pi l/\lambda = 2\pi fl/v \quad (1)$$

Therefore, a wave that propagates at constant velocity can experience a phase shift as seen in (1) by inducing a frequency or transmission line length change. In this manner, an electronic phase shift ( $\psi$ ) is easily generated. Since no phase shifting devices are required, there is no insertion loss due to phase shifters. The series feed arrangement is illustrated in Fig 1. If the beam is to point in a direction  $\theta_0$ , the phase difference between elements should be  $kdsin(\theta_0)$ .

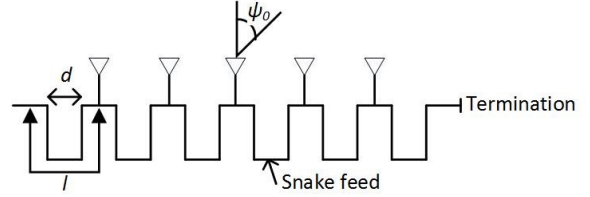


Fig. 1. Elimination of phase shifter using a snake feed.

In scanned arrays, an integral number of  $2\pi$  radians is added which permits a scan angle to be obtained with a smaller frequency change. Equating phase difference to phase shift obtained from a line of length  $l$  gives

$$2\pi d \sin \theta_0 / \lambda + 2\pi m = 2\pi l / \lambda \quad (2)$$

$$\sin \theta_0 = -m\lambda/d + l/d \quad (3)$$

When  $\theta_0=0^\circ$ , which corresponds to the broadside beam direction, (3) results in  $m=l/\lambda_0$ , where  $\lambda_0$  corresponds to the wavelength and  $f_0$  is the center frequency at the broadside direction. Using this information, one can rewrite (3) as

$$\sin \theta_0 = l/d(1 - \lambda/\lambda_0) = l/d(1 - f_0/f) \quad (4)$$

It follows that by changing the length of the water stream, beam steering as a function of phase is achievable with sea water arrays.

## III. SIMULATIONS AND THEORETICAL METHODOLOGY

The array factor of a four element array in sum mode is provided in (5) where  $k$  is the wave number and  $d_x$  and  $d_z$  are the element spacing in the  $x$  and  $z$  axis, respectively. Fig. 2 shows the element pattern for a 4 element array. Illustrations of the array pattern and the total pattern are shown in Fig. 3. A four element array is an equivalent model for our two element sea water array as will be described in the next section.

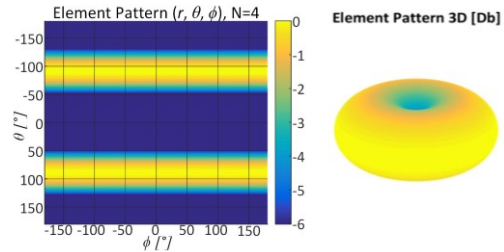


Fig. 2. Element pattern shown in spherical (left) and Cartesian coordinates (right).

$$AF_{\Sigma\text{-beam}} = \sum_{n=1}^4 e^{jk(\hat{r} \cdot \vec{r}_n)} = \left( e^{jk(d_x \sin \theta \cos \phi + d_z \cos \theta)} + e^{-jk(d_x \sin \theta \cos \phi + d_z \cos \theta)} \right) \left( e^{jk(d_x \sin \theta \cos \phi - d_z \cos \theta)} + e^{-jk(d_x \sin \theta \cos \phi - d_z \cos \theta)} \right) \quad (5)$$

$$4 \cos(d_x \sin \theta \cos \phi + d_z \cos \theta) \cos(d_x \sin \theta \cos \phi - d_z \cos \theta)$$

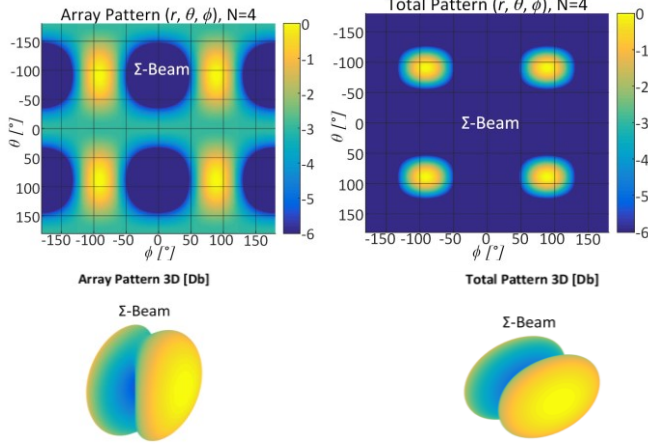


Fig. 3. Sum beam steered to  $\theta=\phi=90$ ; Array pattern (left), total pattern (right),  $(r, \theta, \phi)$  - top and  $(x, y, z)$  - space bottom.

#### IV. DESIGN AND MEASUREMENT ANALYSIS

The sea water “field goal” array was fabricated by connecting two ‘L’ shaped polyvinyl chloride (PVC) tubes together to a central base and filling the structure with seawater. A current probe was connected to the base as an excitation source. The effective wavelength of seawater is provided in (6) whereas the wavelength of free space is provided in (7). Since air was the dominant medium in this experiment it was chosen as the effective wavelength.

$$\lambda_{\text{seawater}} = c/(f\epsilon_r) = c/(80f) \quad (6)$$

$$\lambda_{\text{air}} = c/(f\epsilon_r) = c/f = \lambda_{\text{effective}} \quad (7)$$

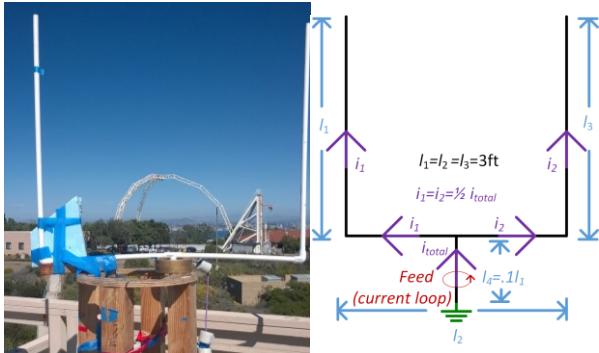


Fig. 4. Sea water field goal element (mechanical rotation).

We designed the center frequency ( $f_0$ ) of the array to be 150 MHz. The element spacing along the  $x$ -axis is calculated as  $0.5\lambda$ . This spacing or line length difference causes a phase cancellation, resulting in two vertical elements (monopoles) of equal phase. The antenna array was measured in an outdoor range as shown in Fig. 4. Also an image current of the sea

water exists due to the placement over the semi perfect lossy earth. This image plane “adds” two additional elements to the array corresponding to a 4-element array (Fig. 5).

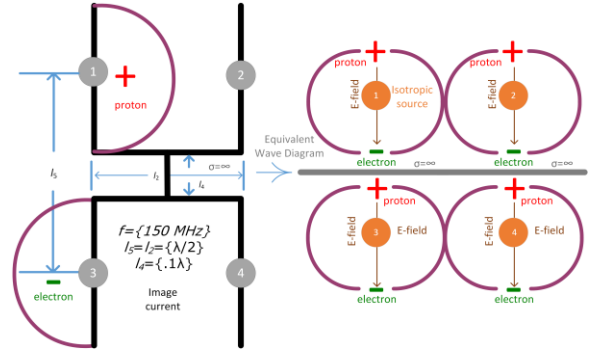


Fig. 5. Equivalent sum ( $\Sigma$ )-beam circuit.

The antenna pattern of the field goal sea water antenna array is shown in Fig. 6. The seawater antenna array was manually positioned at  $0^\circ$ ,  $120^\circ$ , and  $240^\circ$  (relative to the boresight position of the receiving antenna) and excited for transmission. The radiation pattern was measured at each position and the results of the measurement show encouraging agreement with theoretical pattern behavior in Fig. 3.

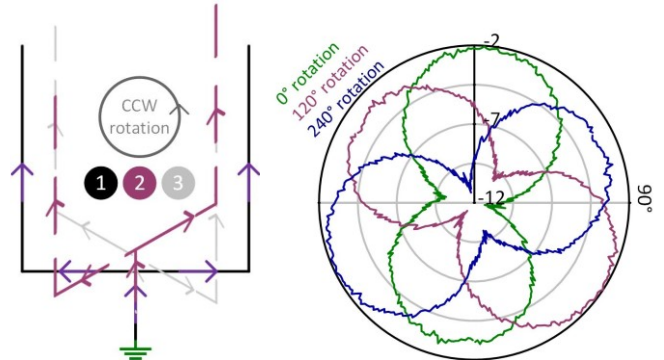


Fig. 6. Measured pattern with three  $120^\circ$  element rotations.

#### V. CONCLUSION

A two element sea water antenna array was fabricated and its antenna pattern measured. The measured patterns show good agreement with simulated results. In addition, the results provide promising validation that future designs of a phase steerable seawater array are possible.

#### REFERENCES

- [1] C. Hua, Z. Shen and J. Lu, "High-Efficiency Sea-Water Monopole Antenna for Maritime Wireless Communications," *IEEE Trans. Antennas and Propag.*, vol. 62, pp. 5968-5973, Dec. 2014.
- [2] Y. Kosta, "Liquid antenna", in *IEEE Antennas and Propagation Society Int. Symp.*, vol. 3, pp. 2392-2395.
- [3] K. Buchanan and G. Huff, "A stochastic mathematical framework for the analysis of spherically bound random arrays," *IEEE Trans. Antennas Propag.*, vol. 62., pp. 3002-3011, June 2014.
- [4] K. R. Buchanan, "Theory and applications of aperiodic (random) phased arrays," Ph.D. dissertation, Dept. Elect. & Com. Eng., Texas A&M University, TX, 2014.